J Pharm Biopharm Res, 2023, 5(1): 366-381
DOI: 10.25082/JPBR.2023.01.002

RESEARCH ARTICLE

Network pharmacology-based prediction for therapeutic mechanism of FuYueKang Lotion on acute eczema

Xiaowen Wen[1] **Shaokang Cui**[2] **Minzhi Li**[3] **Yongping Zheng**[3] **Haoyou Xu**[4*]

[1] Department of Dermatology, Shenzhen Hospital of Guangzhou univercity of Chinese Medicine(futian), Shenzhen 518000, China
[2] Equipment division, Zhongshan Hospital of Traditional Chinese Medicine, Guangzhou 528400, China
[3] Department of Dermatology, Zhongshan Hospital of Traditional Chinese Medicine, Guangzhou 528400, China
[4] Department of Neurology, Guangdong Provincial Hospital of Chinese Medicine, Guangzhou 510120, China

Correspondence to: Haoyou Xu, Guangdong Provincial Hospital of Chinese Medicine, the Second Affiliated Hospital of Guangzhou University of Chinese Medicine, Guangzhou, Guangdong, China;
Email: xuhaoyou@gzucm.edu.cn

Received: August 30, 2023;
Accepted: October 28, 2023;
Published: November 1, 2023.

Citation: Wen X, Cui S, Li M, *et al*. Network pharmacology-based prediction for therapeutic mechanism of FuYueKang Lotion on acute eczema. *J Pharm Biopharm Res*, 2023, **5**(1): 366-381.
https://doi.org/10.25082/JPBR.2023.01.002

Abstract: Objective: Fuyuekang Lotion (FYKL) is an improved traditional Chinese medicine (TCM) prescription widely used to treat acute eczema (AE). However, the mechanism of action remains unclear. This study aimed to explore the therapeutic mechanism of FYKL in AE. Methods: We revealed the underlying mechanism by utilizing a network pharmacology approach, molecular docking studies, and in vitro verification. The active compounds in FYKL were identified, and their targets were predicted. These targets were subsequently mapped to a component-target interaction network, with their therapeutic mechanisms predicted through Gene Ontology (GO) and Kyoto Encyclopedia of Genes and Genomes (KEGG) enrichment analyses. Molecular docking was used to verify protein-binding efficacy. Potential key targets of FYKL against AE were further confirmed via reverse transcription quantitative polymerase chain reaction (RT-qPCR). Results: The study identified 59 potential active compounds of FYKL, with quercetin, luteolin, and gallic acid suggested as critical active ingredients. Our findings suggest that these ingredients could exert their effects mainly by modulating the inflammatory immune response and promoting epidermal repair. FYKL was found to be a multi-target, multi-component drug that could potentially regulate the inflammatory immune response in AE through numerous pathways. Conclusions: The findings from this study provide a scientific basis for further research into the therapeutic effects and mechanisms of FYKL in treating AE, underscoring the potential of TCM in modern therapeutics.

Keywords: Fuyuekang Lotion, acute eczema, network pharmacology, molecular docking, Traditional Chinese medicine

1 Introduction

Acute eczema (AE) is a pervasive inflammatory skin condition characterized by symptoms such as rash, exudates, and severe pruritus. Recent studies have documented an uptick prevalence of 1.1% [1]. Although not life-threatening, AE significantly impairs both mental and physical well-being, and has emerged as one of the most economically burdensome dermatological conditions [2, 3]. Existing clinical guidelines largely endorse the application of topical glucocorticoids as primary therapeutic intervention for AE, however, the potential benefits are frequently offset by an almost equivalent magnitude of adverse reactions [4]. Consequently, a deeper understanding of the pathophysiology of AE and the development of novel preventive strategies are crucial.

Traditional Chinese Medicine (TCM) has a long-standing history of application in the prophylaxis and treatment of AE, with increasing acceptance due to its mild side effects profiles [5, 6]. Fuyuekang lotion (FYKL), an improved herbal formulation developed to address the primary symptoms of AE, is a specific remedy for Zhongshan Traditional Chinese Medicine Hospital. The formulation includes an array of Chinese medicinal herbs, namely Dictamni Cortex (BXP), Sophorae Flavescentis Radix (KS), Platycladi Cacumen (CBY), Schizonepetae Herba (JJ), Phyllanthus emblica L. (GDZJP), Kochiae Fructus (DFZ), Pseudolaricis Cortex (TJP), and Alum (MF). Within the TCM paradigm, AE is construed as “dampness and heat”, and “wind and heat accumulation”syndromes; hence, the herbs present in FYKL work collectively to dispel heat, eliminate dampness, dispel wind-heat and alleviate pruritus. Current pharmacological investigations reveal that the medicinal herbs in FYKL potentially recalibrate the equilibrium of T-helper (Th)1/Th2 cells [7] attenuate skin inflammatory responses, and enhance the recuperation of skin function [8, 9]. Clinical trials have shown the efficacy of FYKL in mitigating edema, erythema, exudates, and other cutaneous inflammatory lesions, thereby ameliorating

clinical manifestations [10]. However, the bioactive components of FYKL and its mechanistic underpinnings in treating AE have yet to be fully elucidated.

The pathogenesis of AE is regarded as being complex and multifactorial, entailing various cellular and molecular signaling pathways. Network pharmacology as a new discipline within systems biology, is poised to decipher the intricate pharmacological mechanisms of TCM formulations [11]. By synergizing pharmacokinetics and pharmacodynamics, network pharmacology enables a comprehensive exploration of the interrelationships among diseases, genes, and medicinal formulations [12].

The present study aimed to predict the active compounds and molecular targets of FYKL that are involved in the alleviation of AE. The ingredients of FYKL and their associated targets were mined from multiple databases and relevant literature. Common targets were identified by aligning compounds and disease targets, and a component-target interaction was subsequently constructed. Further validation was accomplished through Gene Ontology (GO) and pathway enrichment analysis. Moreover, an integrative AE pathway and molecular docking were utilized to expound the potential efficacy of FYKL in mitigating AE pathogenesis at the molecular level, thereby providing direction for further investigation and proposing a new approach to modernizing TCM. Ultimately, the differential expression of key targets was validated through in vitro experiments. The workflow is shown in Figure 1.

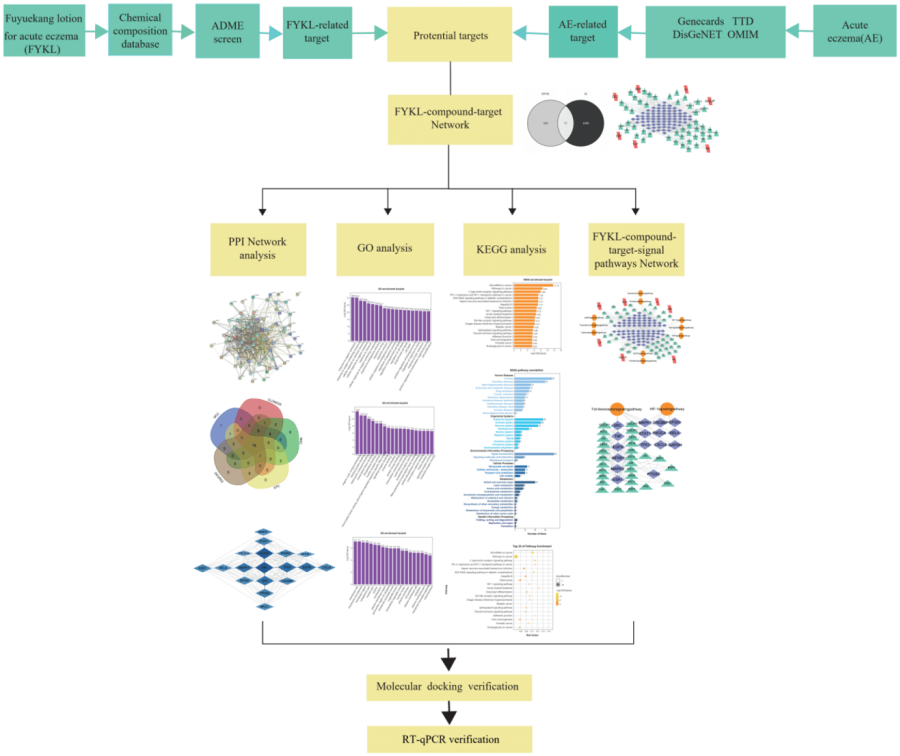

Figure 1 Flowchart of network pharmacology and Verification of FYKL targets against AE

2 Materials and methods

2.1 Database of FYKL ingredients

The chemical ingredients of FYKL, as well as relevant small molecule compounds and their molecular weights, were collated from the TCMSP (https://tcmspw.com/tcmsp.php) [13] and TCMID (http://www.megabionet.org/tcmid/) databases [14]. The structures of small molecule compounds validated through the PubChem database (https://pubchem.ncbi.nlm.nih.gov/) [15] were considered as reference standards. Moreover, their PubChem (https://www.ncbi.nlm.nih.gov/pccompound/?term=) CIDs were used to download structural data files.

2.2 Active ingredients and target protein screening

Active ingredients of FYKL were screened based on the absorption, distribution, metabolism, excretion, and toxicity (ADMET) parameters [16] using the Admet Descriptors module in Discovery Studio 2017R2. Human intestinal absorption indicators considered were ADMET_Absorption_Level and ADMET_Solubility_Level. Prospective active ingredients were

screened by setting prior and posterior values at 0–2 and 1–4, respectively, and ingredients matching these criteria were further analyzed.

Based on the SMILES structures of potential active ingredients, target proteins were obtained *via* DrugBank (https://go.drugbank.com/) [17], the Therapeutic Target Database (TTD, http://db.idrblab.net/ttd/) [18] and the Swiss Target Prediction Platform (STP; http://www.swisstar get prediction.ch/) [19], restricting the species limited to "*Homo sapiens*", and selecting with P $>$ 0.9 criterion. Furthermore, we scored each compound and target, computed network topological parameters from results referencing previous studies [20], deep learning, and Bayesian network algorithms, and identified the targets of the active ingredient in FYKL.

2.3 Identification of AE-related targets in FYKL

The AE-related targets were derived by integrating data from GeneCards (https://www.GeneCards.org/) [21], DisGeNet (https://www.disgenet.org/) [22], Online Mendelian Inheritance in Man (OMIM; https://www.omim.org) [23] , and the Therapeutic Target Database (TTD; http://db.idrbla b.net/ttd/). These databases were searched using "acute eczema" as the keyword, with species limited to 'Homo sapiens.' Genes sourced from GeneCards with quality scores $\geq$ 2.337 and genes obtained from the Comparative Toxigenomics Database (CTD; http://ctdbase.org/)-human) [24] were designated as AE-related. Subsequently, a disease target database was compiled by choosing overlapping targets and removing duplicates or invalid entries.

2.4 Construction of Protein-Protein Interaction (PPI) network and recognition of hub genes

AE-related targets were processed through the STRING database [25] (https://string-db.org/) to construct a protein-protein interaction (PPI) network. Known and predicted protein interactions were identified using STRING based on experimental data, bioinformatic prediction, and literature mining from PubMed abstracts. This approach included 2,031 species, 9.6 million proteins, and 138 million PPIs.

To analyze the potential biological processes (BPs) of the targets in the network, we imported selected data were imported into cytoHubba [26], a Cytoscape 3.8.2 plug-in [27], to predict core protein nodes and subnetworks. Hub genes were filtered using parameters such as degree correlation, maximum neighborhood component, maximum group centrality, edge penetration component, and proximity centrality. The results were then visualized, and clusters of differentially expressed genes were analyzed using the MCODE plug-in [28].

2.5 Functional enrichment analysis

Gene Ontology (GO) and Kyoto Encyclopedia of Genes and Genomes (KEGG) were used to analyze potentially involved BPs, molecular functions (MFs), cellular components (CCs), and signal pathways that might be significantly enriched through key targets. All hub genes were imported into DAVID version 6.8 (https://david.ncifcrf.gov/) [29] for GO and KEGG pathway analysis, restricting the species to "Homo sapiens" and using P $<$ 0.05 as the criterion. The results were visualized and integrated using Cytoscape.

2.6 Construction of component-target-pathway interaction network

Component-target-pathway datasets were imported into Cytoscape (version 3.8.2) to construct a PPI network to explore the multiple components, potential targets, and the pathways of FYKL action against AE. The network comprised the active ingredients, target proteins, and pathways corresponding to the FYKL prescription. The "node" in this network represented an active ingredient of FYKL or an associated target for treating AE, and the "edge" represented the interaction relationship.

2.7 Molecular docking of key targets and components

The Discovery Studio 2017 R2 [30] is a molecular modeling application that can simulate docking and predict key targets and active ingredients in TCMs. The 3D structures of small molecule compounds in the main active ingredients were downloaded from the PubChem database based on their PubChem_ID, and imported into Discovery Studio 2017 R2. High-resolution crystal structures of key target proteins were downloaded from the Protein Data Bank (PDB) [31] (https://www.rcsb.org/). The active domain was set as the corresponding "activity pocket" through the CDOCKER module [32] in Receptor-Ligand International of Discovery Studio 2017 R2, then we searched

and targeted the 'active pocke' near the active site was searched and targeted. The threshold values for the CDOCKER algorithm module were: Pose Clustering Radius = 0.5 and Random Conformations and Orientations to Refine = 10, while all other parameters were kept default.

2.8 Cell culture

HaCat cells were cultured in DMEM with 15% fetal bovine serum (FBS) and maintained at 37°C in 95% air and 5% CO_2. Cells were regularly passaged routinely when cultured to 80-90% confluency and dissociated with trypsin-EDTA (0.25%, Sigma). Before treatment, the cells were synchronized by DMEM medium containing 0.1% FBS. All subsequent experiments were then performed. AE cell model was established by treating cells with 10ug/ml LPS for 24 hours, followed by 5mM ATP for 1 hour [33].

2.9 Real-Time quantitative PCR

Total RNA from HaCat cells was extracted with Trizol, and the RNA concentration was determined using a Bio-Rad quantitative PCR kit (Takara, Japan). The PCR primer sequences are listed in Supplemental Table 1, with β-actin was utilized as the endogenous control.

Table 1 Primer sequences for qRT-PCR

Primer	Sequences (5'→ 3')
h-β-actin	Forward:5′-CATGTACGTTGCTATCCAGGC-3′ Reverse:5′-CTCCTTAATGTCACGCACGAT-3′
H-TNF	Forward:5′-GAGGCCAAGCCCTGGTATG-3′ Reverse:5′-CGGGCCGATTGATCTCAGC-3′
H-β-actin	Forward:5′-ACAACTTTGGTATCGTGGAAGG-3′ Reverse:5′-GCCATCACGCCACAGTTTC-3′
H-TP53	Forward:5′-CAGCACATGACGGAGGTTGT-3′ Reverse:5′-TCATCCAAATACTCCACACGC-3′
H-EGFR	Forward:5′-CAGAGACCCACACTACCAGG-3′ Reverse:5′-ATTTGGCTTGGCTTCCTTGG-3′
H-SRC	Forward:5′-GACAGGCTACATCCCCAGC-3′ Reverse:5′-CGTCTGGTGATCTTGCCAAAA-3′
H-MAPK3	Forward:5′-CTACACGCAGTTGCAGTACAT-3′ Reverse:5′-CAGCAGGATCTGGATCTCCC-3′
H-PTGS2	Forward:5′-CTGGCGCTCAGCCATACAG-3′ Reverse:5′-CGCACTTATACTGGTCAAATCCC-3′
H-ESR1	Forward:5′-GGGAAGTATGGCTATGGAATCTG-3′ Reverse:5′-TGGCTGGACACATATAGTCGTT-3′
H-STAT1	Forward:5′-CGGCTGAATTTCGGCACCT-3′ Reverse:5′-CAGTAACGATGAGAGGACCCT-3′
H-CXCL8	Forward:5′-ACTGAGAGTGATTGAGAGTGGAC-3′ Reverse:5′-AACCCTCTGCACCCAGTTTTC-3′
H-EP300	Forward:5′-GCTTCAGACAAGTCTTGGCAT-3′ Reverse:5′-ACTACCAGATCGCAGCAATTC-3′
H-PPARG	Forward:5′-TACTGTCGGTTTCAGAAATGCC-3′ Reverse:5′-GTCAGCGGACTCTGGATTCAG-3′
H-CREBBP	Forward:5′-CGGCTCTAGTATCAACCCAGG-3′ Reverse:5′-TTTTGTGCTTGCGGATTCAGT-3′
HELA	Forward:5′-CCCACGAGCTTGTAGGAAAGG-3′ Reverse:5′-GGATTCCCAGGTTCTGGAAAC-3′
H-MAPK1	Forward:5′-TCACACAGGGTTCCTGACAGA-3′ Reverse:5′-ATGCAGCCTACAGACCAAATATC-3′
H-NR3C1	Forward:5′-ATAGCTCTGTTCCAGACTCAACT-3′ Reverse:5′-TCCTGAAACCTGGTATTGCCT-3′
H-NFKB1	Forward:5′-AACAGAGAGGATTTCGTTTCCG-3′ Reverse:5′-TTTGACCTGAGGGTAAGACTTCT-3′
H-PIK3CA	Forward:5′-CCACGACCATCATCAGGTGAA-3′ Reverse:5′-CCTCACGGAGGCATTCTAAAGT-3′

3 Results

3.1 Active ingredients in FYKL

We identified 82 related compounds within FYKL from the databases. Using the ADME thresholds and DS software, 59 active ingredients were screened out (BXP, n = 9; DFZ, n = 3; KS, n = 28; JJ, n = 6; CBY, n = 4; TJP, n = 5; GDZJP, n = 4; alum, n = 0). Supplemental Table 2 contains rudimentary information concerning these 59 active ingredients present in FYKL.

Table 2 The active ingredients and ADME parameters of FYKL

NO.	Compound	PubChem CID	ADMET SOLUBLITY level	ADMET absorption level	Herb
BXP1	7alpha-acetylobacunol	57390140	2	0	BXP
BXP2	Isomaculosidine	3083609	3	0	BXP
BXP3	luteolin	5280445	3	0	BXP
BXP4	Obacunone	119041	2	0	BXP
BXP5	preskimmianine	12305721	3	0	BXP
BXP6	quercetin	5280343	3	1	BXP
BXP7	Skimmianin	6760	3	0	BXP
BXP8	trichirubine,b	10392982	2	0	BXP
BXP9	wogonin	5281703	3	0	BXP
KS1	(-)-14beta-hydroxymatrine	10659287	3	0	KS
KS2	(+)-14alpha-hydroxymatrine	15385683	3	0	KS
KS3	(+)-9alpha-hydroxymatrine	15385684	4	0	KS
KS4	(+)-allomatrine	7000681	3	0	KS
KS5	(+)-lehmannine	3041752	3	0	KS
KS6	(+)-Lupanine	91471	3	0	KS
KS7	(2R)-5,7-dihydroxy-2-(4-hydroxyphenyl) chroman-4-one	667495	3	0	KS
KS8	5,7-dihydroxy-2-(3-hydroxy-4-methoxyphenyl) chroman-4-one	676152	3	0	KS
KS9	8-Isopentenyl-kaempferol	1.3E+08	3	0	KS
KS10	anagyrine	442938	3	0	KS
KS11	cis-Dihydroquercetin	443758	3	1	KS
KS12	formononetin	5280378	3	0	KS
KS13	Glyceollin	162807	2	0	KS
KS14	Inermin	91510	2	0	KS
KS15	kushenin	5318889	3	0	KS
KS16	kushenol,t	10598514	2	2	KS
KS17	leachianone,g	25201713	2	0	KS
KS18	Lehmanine	3041752	3	0	KS
KS19	luteolin	5280445	3	0	KS
KS20	matrine	91466	3	0	KS
KS21	Norartocarpetin	5481970	3	0	KS
KS22	Phaseolin	91572	2	0	KS
KS23	quercetin	5280343	3	1	KS
KS24	sophocarpine	115269	3	0	KS
KS25	Sophoramine	169014	3	0	KS
KS26	sophoridine	165549	3	0	KS
KS27	trifolrhizin	442827	3	1	KS
KS28	Wighteone	5281814	2	0	KS
JJ1	5,7-dihydroxy-2-(3-hydroxy-4-methoxyphenyl) chroman-4-one	676152	3	0	JJ
JJ2	Diosmetin	5281612	3	0	JJ
JJ3	luteolin	5280445	3	0	JJ
JJ4	quercetin	5280343	3	1	JJ
JJ5	Schizonepetoside B	5248526	4	0	JJ
JJ6	Schkuhrin I	5281471	3	0	JJ
CBY1	Hinokinin	442879	2	0	CBY
CBY2	Isopimaric acid	442048	2	0	CBY
CBY3	kaempferol	5280863	3	0	CBY
CBY4	quercetin	5280343	3	1	CBY
TJP1	5,8,2'-Trihydroxy-7-methoxyflavone	156992	3	0	TJP
TJP2	Acacetin	5280442	3	0	TJP
TJP3	baicalein	5281605	3	0	TJP
TJP4	Carthamidin	188308	3	0	TJP
TJP5	Coptisine	72322	2	0	TJP
GDZJP1	Ethyl gallate	13250	4	0	GDZJP
GDZJP2	gallic acid	370	4	0	GDZJP
GDZJP3	Methyl gallate	7428	4	0	GDZJP
GDZJP4	trochol	72326	1	1	GDZJP
DFZ1	9E,12Z-octadecadienoic acid	5282798	2	1	DFZ
DEZ2	oleanolic acid	10494	1	1	DFZ
DFZ3	oleic acid	445639	2	2	DFZ

3.2 Compound-target interaction network

We identified 297 FYKL-related targets based on the 59 active ingredients and the target databases. To identify AE-related genes, target data concerning AE from the GeneCards, OMIM, DisGeNET, and TTD databases were compiled, and targets with quality scores surpassing 2.337 were selected as AE-related genes. After merging and deduplication, we screened 1,126 AE-related targets. The intersection of FYKL-related targets and AE-related targets was used to construct a Venn diagram (Figure 2A), resulting in 77 intersectional genes. Subsequently, an FYKL-compound-target interaction network was constructed utilizing these 77 genes, denoted as underlying effective targets for AE treatment (Figure 2B).

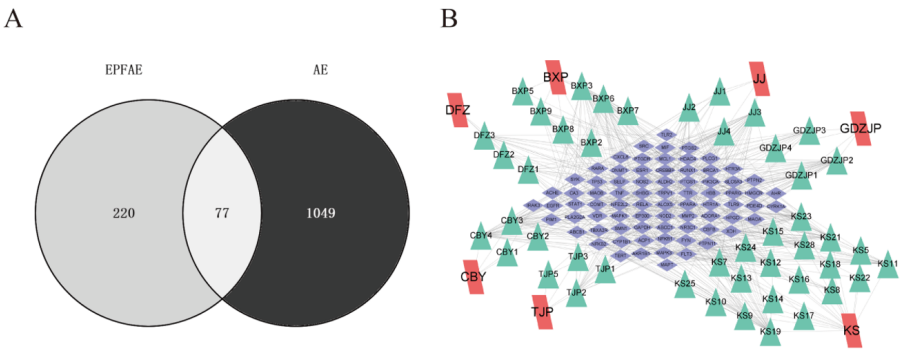

Note: Venn diagram of FYKL targets and AE-related targets (B) Interaction network among FYKL, compounds, and drug targets. Red quadrangle, herbs in FYKL; green triangle, main compound; purple rhombus, drug-related target.

Figure 2 Interaction network analysis of targets

3.3 Construction of PPI network and identification of key targets

A Protein-Protein Interaction (PPI) network was assembled employing Cytoscape to identify key therapeutic targets. Figure 3A demonstrates that the PPI network comprised 76 nodes and 645 edges, in which each node represents a target protein, and edges represent the interaction amongst proteins. The network structure and the weightage between nodes of the PPI were analyzed using the five cytoHubba algorithms in Cytoscape. The intersections of the top 20 targets from each algorithm were reserved as key targets (Figure 3B and Table 3). Figure 3C shows 18 key targets that were analyzed using the topological parameter, with the results demonstrated in Table 4. The top five key targets included tumor necrosis factor (TNF), glyceraldehyde 3-phosphate dehydrogenase (GAPDH), tumor protein (TP) 53, epidermal growth factor receptor (EGFR), and proto-oncogene tyrosine-protein kinase Src (SRC).

Table 3 Ranking of Cytohubba's five-algorithm calculation results

Rank	MCC	CLONESS	MNC	EPC	DEGREE
1	AHR	CREBBP	CREBBP	BRCA1	CREBBP
2	BRCA1	CXCL8	CXCL8	CREBBP	CXCL8
3	CREBBP	EGFR	EGFR	CXCL8	EGFR
4	CXCL8	EP300	EP300	EGFR	EP300
5	EGFR	ESR1	ESR1	EP300	ESR1
6	EP300	GAPDH	GAPDH	ESR1	GAPDH
7	ESR1	MAPK1	MAPK1	GAPDH	MAPK1
8	GAPDH	MAPK3	MAPK3	MAPK1	MAPK3
9	MAPK1	NFKB1	NFKB1	MAPK3	NFKB1
10	MAPK3	NR3C1	NR3C1	NFKB1	NR3C1
11	NFKB1	PIK3CA	PIK3CA	NR3C1	PIK3CA
12	NR3C1	PPARG	PPARG	PIK3CA	PPARG
13	PIK3CA	PTGS2	PTGS2	PPARG	PTGS2
14	PPARG	RELA	RELA	PTGS2	RELA
15	PTGS2	SRC	SRC	RELA	SRC
16	RELA	STAT1	STAT1	SRC	STAT1
17	SRC	SYK	SYK	STAT1	SYK
18	STAT1	TLR2	TLR2	TLR2	TLR2
19	TNF	TNF	TNF	TNF	TNF
20	TP53	TP53	TP53	TP53	TP53

Table 4 Topological parameters of key targets

Name	Closeness	Betweenness	Degree
TNF	0.765306	0.126778393	52
GAPDH	0.750000	0.105184808	50
TP53	0.714286	0.06054704	45
EGFR	0.700935	0.066724724	43
SRC	0.700935	0.061078569	43
MAPK3	0.688073	0.034694475	41
PTGS2	0.669643	0.051185854	38
ESR1	0.652174	0.043397778	35
STAT1	0.646552	0.015919872	35
CXCL8	0.641026	0.02088322	34
EP300	0.646552	0.025963376	34
PPARG	0.635593	0.027190811	33
CREBBP	0.6250000	0.02429554	31
RELA	0.6250000	0.007218512	31
MAPK1	0.6250000	0.01822738	30
NR3C1	0.6250000	0.060558609	30
NFKB1	0.590551	0.002849999	24
PIK3CA	0.576923	0.003330178	23

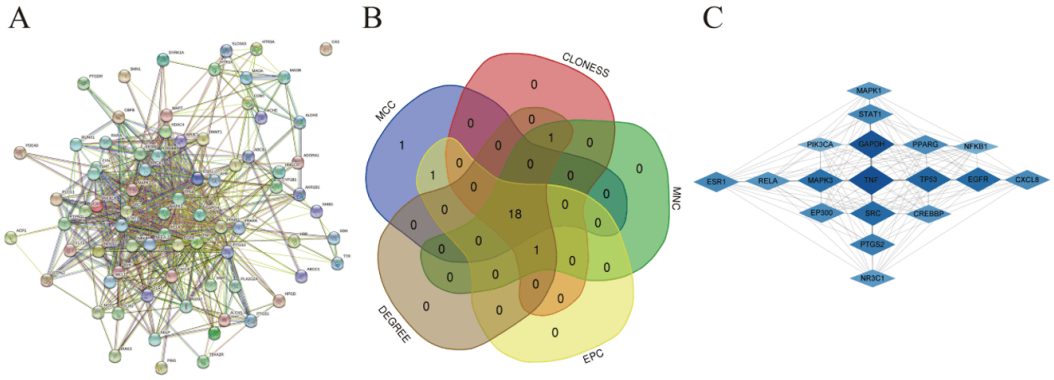

Figure 3 Protein-protein interaction (PPI) network. Protein-protein interaction PPI network of 76 nodes and 645 edges. (B) Venn diagram of top 20 targets among five algorithms (MNC, DEGREE, MCC, CLONESS with EPC). (C) PPI network of key targets.

3.4 Sub-Network analysis

Gene groups with closer connections in a network can be found by analyzing MCODE sub-networks using weighted calculations of the highest weight and a recursive approach. Generally, targets that are closer to the center hold more importance. In sub-network 1, the crucial targets were Nuclear Factor Kappa B Subunit 1 (NFKB1) and TNF, indicating a strong association with the inflammatory response (Figure 4A). In sub-network 2, acetylcholinesterase (ACHE) scored the highest, with the nearby genes monoamine oxidase B (MAOB) and 5-hydroxytryptamine receptor 3A (HTR3A) associated with the nervous system (Figure 4B).

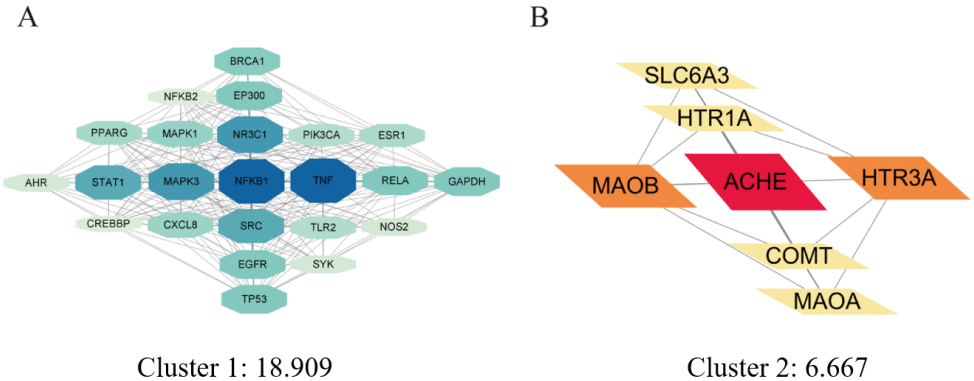

Figure 4 Sub-network. Node sizes and color reflect the score of the target point (degree). Larger nodes and darker-colored nodes have higher scores.

3.5 GO biological enrichment

To gain better comprehension of the interactions amongst common targets, a GO enrichment analysis was carried out using DAVID 6.8 with a screening criterion of $P < 0.05$. As presented in Figure 5 and Table 5, these targets correlate closely with 283 BPs, 92 MFs, and 33 CCs. The core targets in BPs mainly focused on the response to organic substances, response to oxygen-containing compounds, cellular response to chemical stimuli, cellular response to organic substances, and response to chemicals. The MFs were related to organic cyclic compound binding, identical protein binding, heterocyclic compound binding, transcription factor binding, and phosphatase binding; CCs were involved in membrane rafts, membrane microdomains, membrane regions, cytoplasmic parts, and nuclear parts.

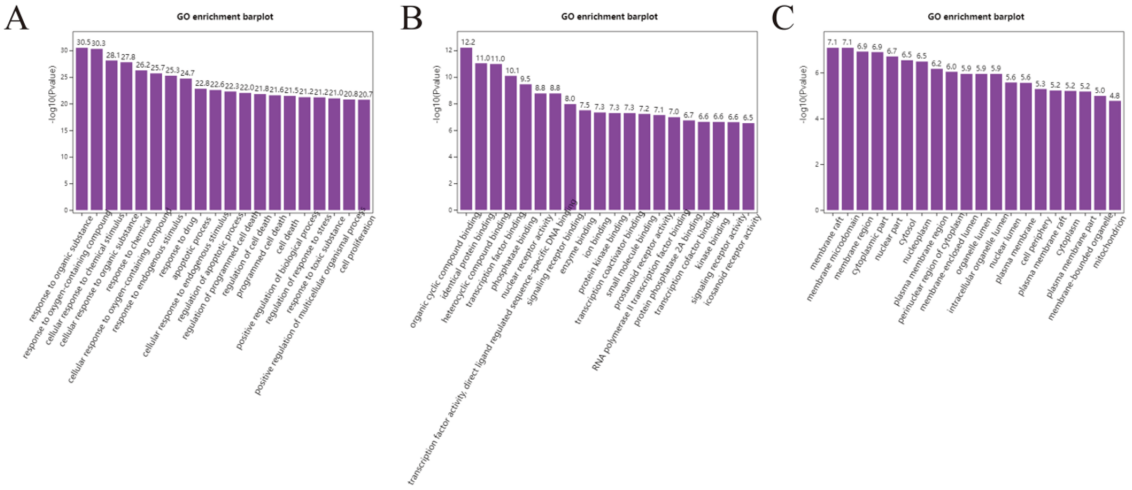

Figure 5 Gene Otology enrichment of 77 key targets. Top 20 terms in each GO category with $p < 0.05$ were selected. (A) Biological process, (B) molecular function, (C) CC analysis of key targets.

Table 5 The active ingredients and ADME parameters of FYKL

Class	GO	term	Count	P-value
Biological Process	GO:0010033	response to organic substance	59	3.24E-31
	GO:1901700	response to oxygen-containing compound	47	5.05E-31
	GO:0070887	cellular response to chemical stimulus	57	7.81E-29
	GO:0071310	cellular response to organic substance	53	1.69E-28
	GO:0042221	response to chemical	63	5.72E-27
	GO:1901701	cellular response to oxygen-containing compound	38	2.12E-26
	GO:0009719	response to endogenous stimulus	43	5.60E-26
	GO:0042493	response to drug	36	1.93E-25
	GO:0006915	apoptotic process	43	1.57E-23
	GO:0071495	cellular response to endogenous stimulus	38	2.79E-23
Molecular Function	GO:0097159	organic cyclic compound binding	54	6.28E-13
	GO:0042802	identical protein binding	31	9.36E-12
	GO:1901363	heterocyclic compound binding	52	1.06E-11
	GO:0008134	transcription factor binding	18	8.27E-11
	GO:0019902	phosphatase binding	11	3.54E-10
	GO:0004879	nuclear receptor activity	7	1.75E-09
	GO:0098531	transcription factor activity, direct ligand regulated sequence-specific DNA binding	7	1.75E-09
	GO:0005102	signaling receptor binding	24	1.10E-08
	GO:0019899	enzyme binding	27	3.22E-08
	GO:0043167	ion binding	48	4.75E-08
Cellular Component	GO:0045121	membrane raft	11	1.29E-05
	GO:0098857	membrane microdomain	11	1.29E-05
	GO:0098589	membrane region	11	1.29E-05
	GO:0044444	cytoplasmic part	61	1.29E-05
	GO:0044428	nuclear part	40	1.59E-05
	GO:0005829	cytosol	42	1.91E-05
	GO:0005654	nucleoplasm	36	1.91E-05
	GO:0098590	plasma membrane region	18	3.45E-05
	GO:0048471	perinuclear region of cytoplasm	14	3.82E-05
	GO:0031974	membrane-enclosed lumen	42	3.82E-05

3.6 KEGG pathway enrichment

We explored the signaling pathways of potential targets using KEGG pathway enrichment via DAVID 6.8. As shown in Table 6, the top 10 pathways of FYKL effects on AE were predominantly associated with the hypoxia-inducible factor (HIF)-1, Toll-like receptor, sphingolipid, thyroid hormone, prolactin, neurotrophin, cAMP, T cell receptor, TNF, and VEGF. These could be considered the key pathways involved in AE treatment (Figure 6).

Table 6 KEGG enrichment pathway

Pathway	Count	*P*-Value
HIF-1 signaling pathway	11	7.58E-09
Toll-like receptor signaling pathway	10	3.23E-08
Sphingolipid signaling pathway	10	1.31E-07
Thyroid hormone signaling pathway	10	1.77E-07
Prolactin signaling pathway	8	3.82E-07
Neurotrophin signaling pathway	9	1.53E-06
cAMP signaling pathway	11	3.83E-06
T cell receptor signaling pathway	8	5.69E-06
TNF signaling pathway	8	6.94E-06
VEGF signaling pathway	6	1.84E-05

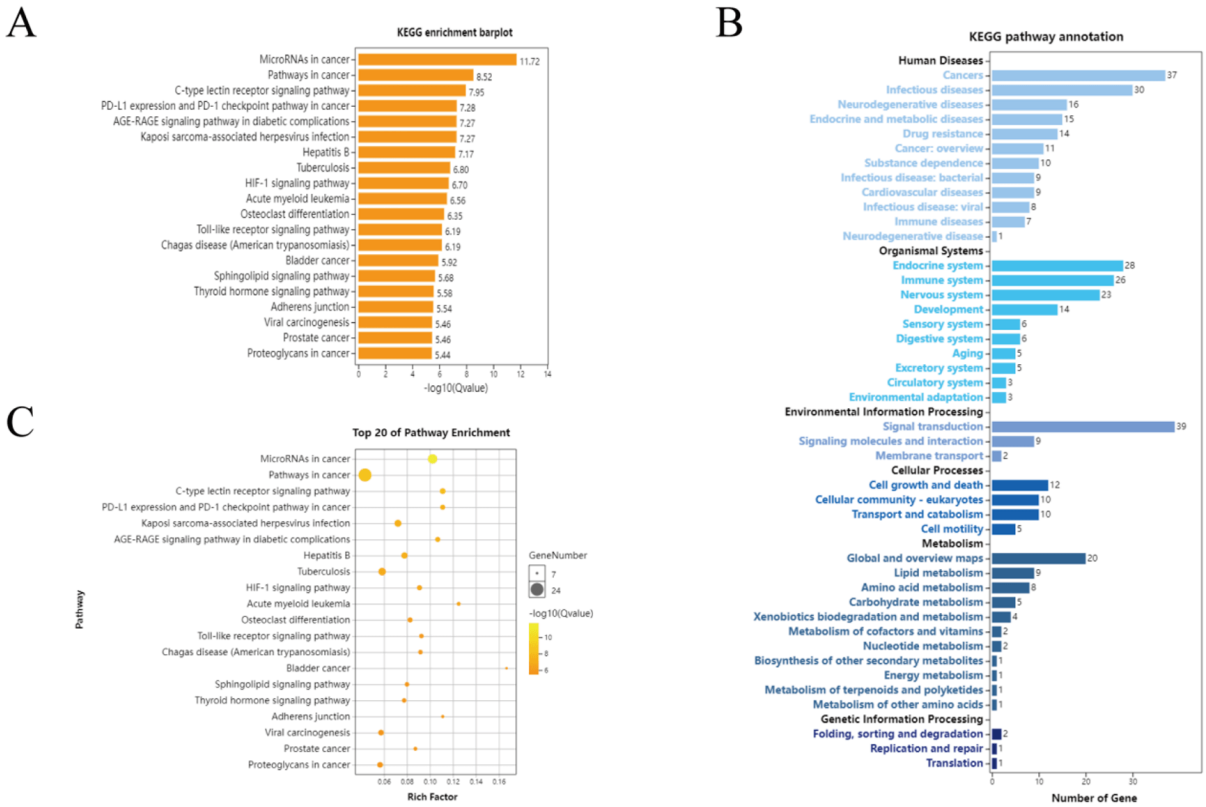

Figure 6 KEGG enrichment analyses. (A) Histogram of KEGG enrichment pathways; (B) Annotated classification of KEGG enrichment pathways; (C) Bubble chart of KEGG enrichment pathways.

3.7 Construction of active ingredients-core targets-pathways network

We conducted further investigations into the potential mechanism of the anti-inflammatory effects of FYKL on AE by constructing an interaction network based on the active compounds in FYKL, the core targets, and the significant KEGG pathways as described in section 3.6 (Figure 7A). The data were imported into Cytoscape 3.8.2, and the closest relationships between active ingredients and core targets were calculated using the cytoHubba plugin. As shown in Figure 7B, the Hypoxia-inducible factor 1 (HIF-1) signaling pathway emerged as core pathway involved in AE treatment. Hypoxia-inducible factor-1 promotes the perception and coordination of hypoxia responses, which play an important role in relieving inflammation [34].

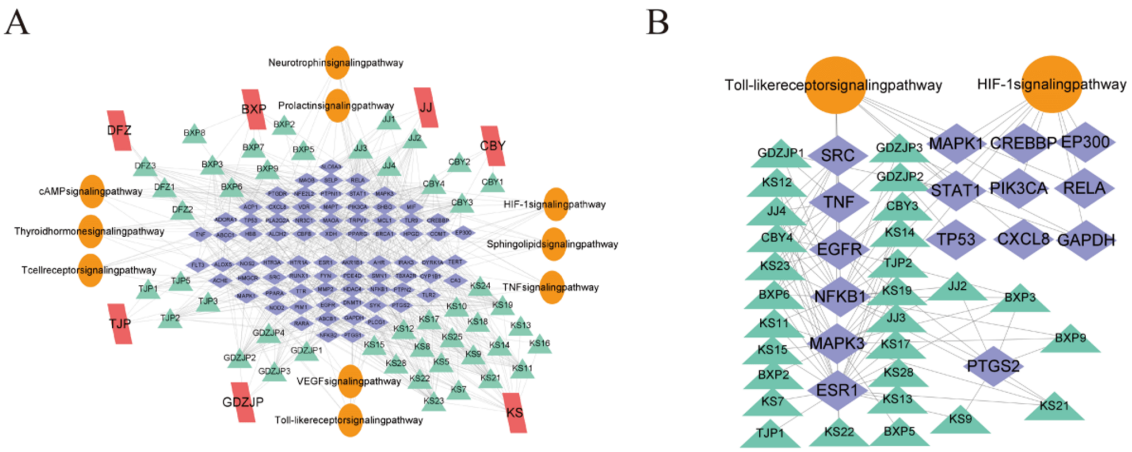

Figure 7 FYKL-component-target-pathway network. (A) Interaction network of FYKL-component-target-pathway. (B) Key targets-components network. Red quadrangle, green triangle, purple diamond, and orange ellipse represent herbs in FYKL, components, targets, and related pathway, respectively.

3.8 Molecular docking verification

To evaluate the binding between the core target and its related compounds, we simulated molecular docking using affinity values. Typically, a lower affinity score indicates a stronger binding effect. The virtual verification results in Table 7 suggest that the molecular docking targets and the core components of FYKL exhibit strong binding activity. Notably, the EGFR and kaempferol pair showed the most robust binding (with an affinity score of -137.87 kcal/mol). Among the docking pairs, those with higher scores were selected for 3D and 2D visualization (Figure 8). These results further emphasize the practicality and clinical feasibility of systems pharmacology.

Table 7 Molecular docking scores between core targets and related compounds

Targets	PDB ID	Compounds	Affinity (kcal/mol)
TNF	2E7A	quercetin	-50.9367
		Ethyl gallate	-53.9928
		Methyl gallate	-47.2006
GAPDH	1U8F	gallic acid	-35.8892
		Methyl gallate	-39.3964
TP53	5HOU	gallic acid	-37.1244
EGFR	5XWD	luteolin	-47.7778
		quercetin	-116.545
		kaempferol	-137.87
		gallic acid	-118.945
SRC	1Y57	quercetin	-38.3636
MAPK3	2ZOQ	luteolin	-38.6381
		quercetin	-57.8526
		wogonin	-29.5942
		Diosmetin	-36.0386
		cis-Dihydroquercetin	-38.5834
		Norartocarpetin	-35.797
PTGS2	5F19	luteolin	-18.155
		wogonin	-11.0298
		Diosmetin	-16.6934
		Norartocarpetin	-16.1364
ESR1	4ZNH	luteolin	-22.6955
		quercetin	-37.218
		kaempferol	-37.1051
		cis-Dihydroquercetin	-25.7716
		Norartocarpetin	-22.6643
STAT1	1YVL	Ethyl gallate	-65.2177
		gallic acid	-60.2225
		Methyl gallate	-65.7285
NFKB1	2O61	Luteolin	-26.3225
		quercetin	-36.5735
		Wogonin	-21.0558
		kaempferol	-52.8953
		Ethyl gallate	-48.6136
		gallic acid	-44.5103
		Methyl gallate	-43.2183
		Diosmetin	-23.9117
		cis-Dihydroquercetin	-26.1675
		Norartocarpetin	-23.5012

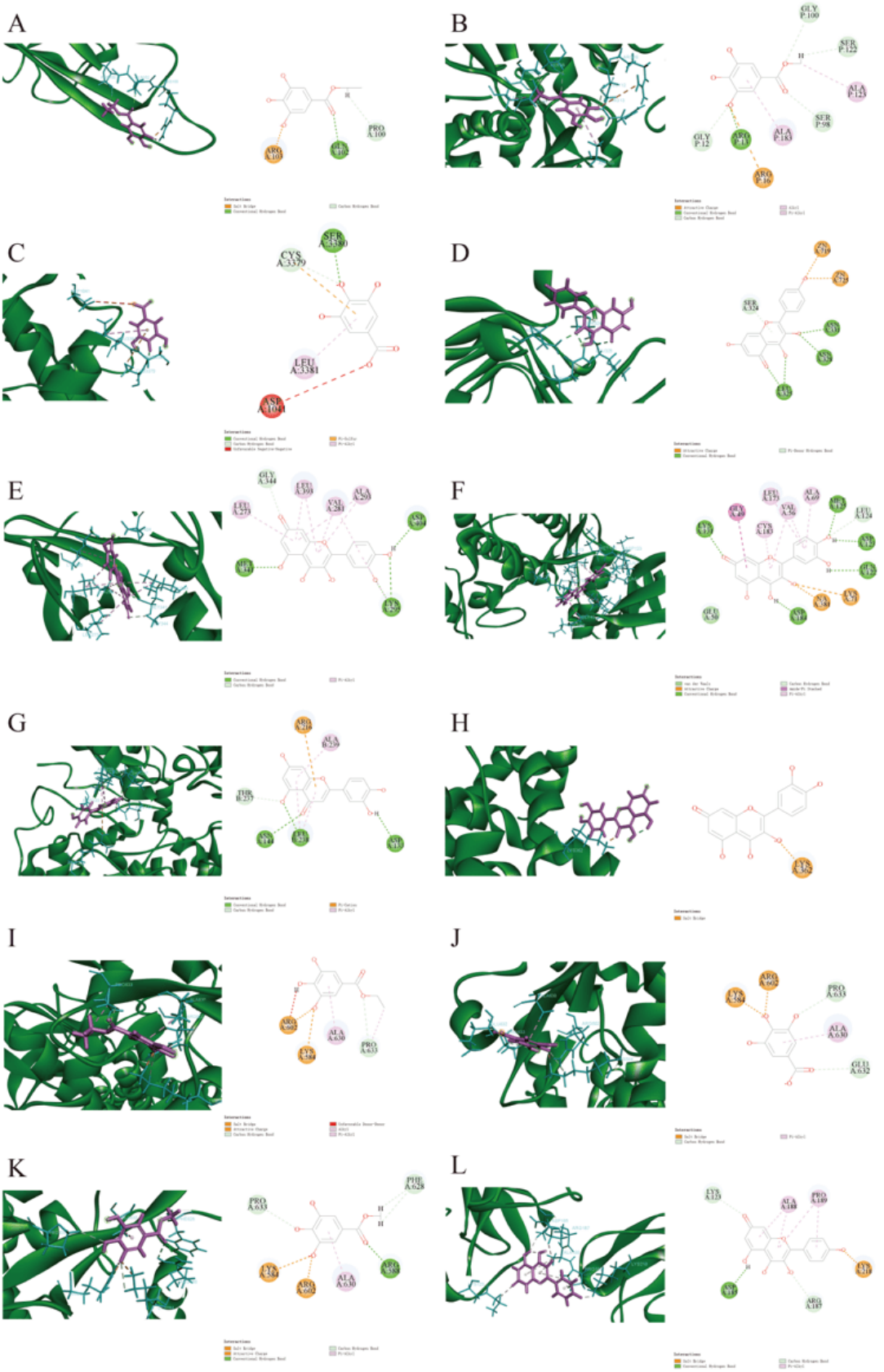

Figure 8 Molecular docking models of representative components-targets. TNF-ethyl gallate. (B) GAPDH-methyl gallate. (C) TP53-gallic acid. (D) EGFR-kaempferol. (E) SRC-quercetin. (F) mitogen-activated protein kinase 3 MAPK3-quercetin. (G) PTGS2-luteolin. (H) ESR1-quercetin. (I) STAT1-ethyl gallate. (J) STAT1-gallic acid. (K) STAT1-methyl gallate. (L) NFKB1-kaempferol.

3.9 Validation of differentially expressed key targets in HaCat cells

To verify the results of network pharmacology and molecular docking in a cell culture context, we established an in vitro model of AE using HaCat cells. The cells were pretreated with LPS for 24 hours, followed by ATP treatment for 1 hour. We measured the expression of 18 potential key targets of FYKL against AE (from Table 4) using RT-qPCR. The results showed that 4 out of the 18 genes (CXCL8, PTGS2, MAPK3, and NR3C1) exhibited increased RNA levels in LPS-treated HaCat cells compared to non-treated control cells. This suggests these 4 genes are crucial in AE development and may be the primary targets of FYKL. (see Figure 9)

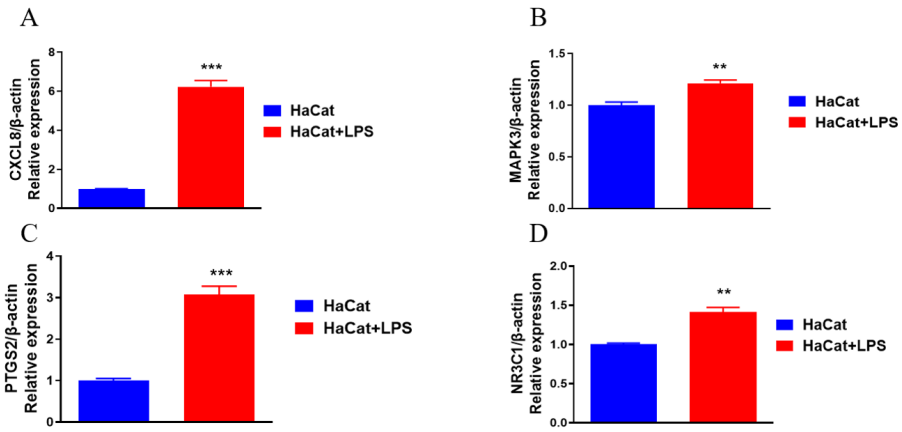

Figure 9 Differential expression of CXCL8(A), MAPK3(B), PTGS2(C), and NR3C1(D) were verified by RT-qPCR in HaCat cells.

4 Discussion

The pathogenesis of acute eczema is complex and multifactorial, encompassing numerous cellular and molecular signaling pathways, network pharmacology provides a systematic analysis approach for researching it. Utilizing multiple bioinformatics databases and literature mining, we analyzed the active ingredients of FYKL and their related targets. We then mapped these predicted targets to a component-target interaction network. Moreover, the therapeutic mechanisms were predicted by analyzing GO and EKGG enrichment and verified protein binding effects through molecular docking and RT-qPCR.

As traditional Chinese medicines, the role and mechanisms of FYKL and its various active ingredients in AE have been frequently reported. Studies have found that FYKL can inhibit DNCB-induced eczema in mice by downregulating key active constituents, such as quercetin [8], luteolin [9], gallic acid [35, 36], and other phenylpropanoid compounds. These compounds have also been shown to inhibit inflammation during the pathogenesis of AE. For instance, quercetin exerts an anti-inflammatory effect by inhibiting the NFkB inflammatory pathway [37] and modulating of extracellular signal-regulated kinase [38]. Additionally, quercetin contributes to skin wound repair in patients [39]. Luteolin is a natural flavonoid compound in KS, JJ, and other herbs, potentially inhibits inflammation by suppressing proinflammatory mediators such as IL-6, TNF-α, and cyclooxygenase-2 (COX-2) and regulating various signaling pathways-mediated [40]. Luteolin also contributes to the regulation of nerve tissue repair, and regeneration processes [41]. Gallic acid is a natural polyphenol organic compound found in many herbs [42]. It attenuates the inflammatory response by inhibiting NF-κB, prostaglandin E2 (PGE2), and MAPK signaling pathways. We previously showed that KS exerts an anti-inflammatory effect on eczema, presumably by regulating the TH1/TH2 balance through inhibiting TGF-β levels. Taken together, these findings suggest that the main active ingredients of FYKL are potential candidate compounds for treating AE.

In this study, we identified 59 active compounds in FYKL, 297 FYKL-related targets, and 1,126 AE-related targets. After gene mapping and constructing a PPI network, we identified 18 intersecting genes. The top five key targets - tumor necrosis factor (TNF), glyceraldehyde 3-phosphate dehydrogenase (GAPDH), tumor protein 53 (TP53), epidermal growth factor receptor (EGFR), and proto-oncogene tyrosine-protein kinase Src (SRC) - are all associated with inflammation. The binding of TNF and GAPDH can lead to the inhibition of inflammation [43, 44], which suggests they participate in the pathogenesis of AE through inflammation regulation. Both TP53 [35] and EGFR [36] are involved in cell proliferation and signal

transduction, and may affect the balance of inflammation. The SRC gene, associated with tumor development [45], may regulate AE-associated signaling as part of its inflammatory activity. Moreover, the results of the sub-network analysis imply that the mechanism of FYKL is closely linked to the inflammatory response, notably involving the Nuclear Factor Kappa B Subunit 1 (NFKB1) and acetylcholinesterase (ACHE). NFKB1, a key activator of inflammation, may help to maintain homeostasis and promote epidermal repair [37]. It is associated with the other main components of FYKL and multiple signaling pathways. ACHE, belonging to an enzyme family involved in biological nerve conduction, may control itching through neuropeptide release and signaling [38]. Thus, inflammation is the dominant pathological mechanism of AE and can exacerbate symptoms. Our data suggest that FYKL may counter this through its active compounds' interaction with multiple targets, and these findings could provide a foundation for further research into FYKL's potential application in AE treatment.

Analyses of GO and KEGG enrichment indicated that FYKL may treat AE by modulating the HIF-1 [46,47] and Toll-like receptor [48] signaling pathways. Both pathways can regulate the release of pro-inflammatory and anti-inflammatory cytokines. Inflammatory stimuli, such as reactive oxygen species, nitrogen species (NO), and cytokines, can lead to vasoconstriction, vascular blockage, and even insufficient blood supply, increasing oxygen consumption in local tissue. As a result, the skin's inflammatory response is often accompanied by a hypoxic microenvironment. An imbalance among intracellular and extracellular inflammatory signaling pathways could activate the adaptive immune response and induce AE development. Activation of the adaptive immune response may help to inhibit the development of infection processes in skin cells by reducing oxygen supply, and the perception and regulation of hypoxia-responsive responses are mainly promoted by the HIF. Further calculations using cytoHubba's MCC algorithm identified the HIF-1 signaling pathway as the key pathway for FYKL's effect. Therefore, we infer that FYKL's alleviation of AE is associated with skin inflammation, immunomodulation, and reversal of the hypoxic microenvironment.

To further validate our network pharmacology predictions, we investigated interactions between the core targets and their corresponding active components using molecular docking. The results showed that all core targets and their related components had good binding energy (affinity below -10 kcal/mol), with two-thirds having even stronger binding energy (affinity below -30 kcal/mol). RT-qPCR results also indicated that the expression of CXCL8, PTGS2, MAPK3, and NR3C1 was misregulated in HaCat cells pretreated with LPS and ATP, further supporting our network pharmacology predictions.

In summary, our study identified quercetin, luteolin and gallic acid as critical active ingredients in FYKL that regulate AE. We demonstrated that these ingredients could mitigate skin inflammation primarily by regulating the inflammatory immune response and promoting epidermal repair. Our in vitro experimental results further supported these findings, as potential targets of FYKL, such as PTGS2, CXCL18, NR3C1 and so on, were indeed misregulated in AE. These results provide a scientific baseline for future experimental research into the mechanism of FYKL's action against AE.

However, we acknowledge that there are limitations to identifying the core active components solely through the results above, as we cannot clearly define the correlation between specific action intensity and efficacy. Therefore, the specific anti-inflammatory mechanism of FYKL in AE, along with the targets and pathways of the active ingredients in the prescription, still require further confirmation.

5 Conclusion

In conclusion, this study explored the therapeutic mechanism of Fengyankangliu (FYKL) in treating acute eczema (AE) by combining network pharmacology, molecular docking, and in vitro verification. The findings suggest that FYKL, as a traditional Chinese medicine formulation, is a multi-component and multi-target drug that may modulate the inflammatory immune response in AE through numerous pathways. The active ingredients of FYKL, such as quercetin, luteolin, and gallic acid, were identified as potential key contributors in the regulation of AE, with their effects linked primarily to the modulation of inflammatory immune responses and the promotion of epidermal repair. The study, however, recognized certain limitations, such as the inability to precisely define the correlation between specific action intensity and efficacy. Therefore, further experimental research is required to confirm the specific anti-inflammatory mechanism of FYKL in AE and the targets and pathways of the active ingredients in the prescription. The approach taken in this study could offer a new way to explain the clinical effects of TCM formulations, potentially contributing to the development and wider acceptance of TCM in contemporary medicine.

Ethical approval

There is no human or animal studies in this study.

Competing interests

All authors declare no conflicts of interest.

Funding support

This work was supported by the Guangdong Provincial PhD Station funding, Zhongshan Social Welfare and Basic Research Project (No. 2021B1063).

Availability of data and materials

All data in this study are available from the corresponding author upon reasonable request.

Abbreviations

ACHE:	acetylcholinesterase
AP-1:	Activator protein 1
COX-2:	Cyclooxygenase-2
FYKL:	Fuyuekang Lotion
HIF-1:	Hypoxia-inducible factor 1
HTR3A:	5-Hydroxytryptamine receptor 3A
IL-6:	Interleukin 6
JAK-STAT:	Janus kinase-signal transducer and activator of transcription
MAOB:	Monoamine oxidase B
MAPK:	Mitogen-activated protein kinase
NF-κB:	Nuclear Factor Kappa B
NFKB1:	Nuclear Factor Kappa B Subunit 1
PGE2:	Prostaglandin E2
PPI:	Protein-protein interaction
TCM:	Traditional Chinese Medicine
TCR:	T-cell receptor
TNF-α:	Tumor necrosis factor alpha
TNFR:	Tumor necrosis factor receptor

References

[1] de Lusignan S, Alexander H, Broderick C, et al. The epidemiology of eczema in children and adults in England: A population-based study using primary care data. Clinical and Experimental Allergy. 2020, 51(3): 471-482. https://doi.org/10.1111/cea.13784

[2] Ellis CN, Drake LA, Prendergast MM, et al. Cost of atopic dermatitis and eczema in the United States. Journal of the American Academy of Dermatology. 2002, 46(3): 361-370. https://doi.org/10.1067/mjd.2002.120528

[3] Hay RJ, Johns NE, Williams HC, et al. The Global Burden of Skin Disease in 2010: An Analysis of the Prevalence and Impact of Skin Conditions. Journal of Investigative Dermatology. 2014, 134(6): 1527-1534. https://doi.org/10.1038/jid.2013.446

[4] Nowicki R, Trzeciak M, Wilkowska A, et al. Special paper Atopic dermatitis: current treatment guidelines. Statement of the experts of the Dermatological Section, Polish Society of Allergology, and the Allergology Section, Polish Society of Dermatology. Advances in Dermatology and Allergology. 2015, 4: 239-249. https://doi.org/10.5114/pdia.2015.53319

[5] Gu SX, Zhang AL, Coyle ME, et al. Chinese herbal medicine granules (PTQX) for children with moderate to severe atopic eczema: study protocol for a randomised controlled trial. Trials. 2015, 16(1). https://doi.org/10.1186/s13063-015-0806-y

[6] Wang Z, Wang ZZ, Geliebter J, Tiwari R, Li XM. Traditional Chinese medicine for food allergy and eczema. Annals of Allergy, Asthma and Immunology. 2021, 126(6): 639-654. https://doi.org/10.1016/j.anai.2020.12.002

[7] Zhang L, Lin S, Zheng Y, Wang H. Matrine Regulates Th1/Th2 Balance to Treat Eczema by Upregulating Interferon-γ. Journal of Nanoscience and Nanotechnology. 2020, 20(6): 3378-3386. https://doi.org/10.1166/jnn.2020.17417

[8] Hwang SJ, Song YS, Lee HJ. Phaseolin Attenuates Lipopolysaccharide-Induced Inflammation in RAW 264.7 Cells and Zebrafish. Biomedicines. 2021, 9(4): 420.
https://doi.org/10.3390/biomedicines9040420

[9] Zhou W, Hu M, Hu J, Du Z, Su Q, Xiang Z. Luteolin Suppresses Microglia Neuroinflammatory Responses and Relieves Inflammation-Induced Cognitive Impairments. Neurotoxicity Research. 2021, 39(6): 1800-1811.
https://doi.org/10.1007/s12640-021-00426-x

[10] Zhang L, Lin S, Zheng Y. Observation on the efficacy of Fuyuekang lotion in the treatment of acute (subacute) eczema. Guangming Traditional Chinese Medicine. 2015, 30(5): 987-988.

[11] Chen S, Jiang H, Cao Y, et al. Drug target identification using network analysis: Taking active components in Sini decoction as an example. Scientific Reports. 2016, 6(1).
https://doi.org/10.1038/srep24245

[12] Zhang R, Zhu X, Bai H, Ning K. Network Pharmacology Databases for Traditional Chinese Medicine: Review and Assessment. Frontiers in Pharmacology. 2019, 10.
https://doi.org/10.3389/fphar.2019.00123

[13] Ru J, Li P, Wang J, et al. TCMSP: a database of systems pharmacology for drug discovery from herbal medicines. Journal of Cheminformatics. 2014, 6(1).
https://doi.org/10.1186/1758-2946-6-13

[14] Xue R, Fang Z, Zhang M, Yi Z, Wen C, Shi T. TCMID: traditional Chinese medicine integrative database for herb molecular mechanism analysis. Nucleic Acids Research. 2012, 41(D1): D1089-D1095.
https://doi.org/10.1093/nar/gks1100

[15] Kim S, Chen J, Cheng T, et al. PubChem 2019 update: improved access to chemical data. Nucleic Acids Research. 2018, 47(D1): D1102-D1109.
https://doi.org/10.1093/nar/gky1033

[16] Ferreira LLG, Andricopulo AD. ADMET modeling approaches in drug discovery. Drug Discovery Today. 2019, 24(5): 1157-1165.
https://doi.org/10.1016/j.drudis.2019.03.015

[17] Law V, Knox C, Djoumbou Y, et al. DrugBank 4.0: shedding new light on drug metabolism. Nucleic Acids Research. 2013, 42(D1): D1091-D1097.
https://doi.org/10.1093/nar/gkt1068

[18] Chen X. TTD: Therapeutic Target Database. Nucleic Acids Research. 2002, 30(1): 412-415.
https://doi.org/10.1093/nar/30.1.412

[19] Daina A, Michielin O, Zoete V. SwissTargetPrediction: updated data and new features for efficient prediction of protein targets of small molecules. Nucleic Acids Research. 2019, 47(W1): W357-W364.
https://doi.org/10.1093/nar/gkz382

[20] Fu X, Mervin LH, Li X, et al. Toward Understanding the Cold, Hot, and Neutral Nature of Chinese Medicines Using in Silico Mode-of-Action Analysis. Journal of Chemical Information and Modeling. 2017, 57(3): 468-483.
https://doi.org/10.1021/acs.jcim.6b00725

[21] Safran M, Dalah I, Alexander J, et al. GeneCards Version 3: the human gene integrator. Database. 2010, 2010(0): baq020-baq020.
https://doi.org/10.1093/database/baq020

[22] Piñero J, Bravo À, Queralt-Rosinach N, et al. DisGeNET: a comprehensive platform integrating information on human disease-associated genes and variants. Nucleic Acids Research. 2016, 45(D1): D833-D839.
https://doi.org/10.1093/nar/gkw943

[23] Hamosh A. Online Mendelian Inheritance in Man (OMIM), a knowledgebase of human genes and genetic disorders. Nucleic Acids Research. 2002, 30(1): 52-55.
https://doi.org/10.1093/nar/30.1.52

[24] Davis AP, Grondin CJ, Johnson RJ, et al. Comparative Toxicogenomics Database (CTD): update 2021. Nucleic Acids Research. 2020, 49(D1): D1138-D1143.
https://doi.org/10.1093/nar/gkaa891

[25] Szklarczyk D, Gable AL, Lyon D, et al. STRING v11: protein–protein association networks with increased coverage, supporting functional discovery in genome-wide experimental datasets. Nucleic Acids Research. 2018, 47(D1): D607-D613.
https://doi.org/10.1093/nar/gky1131

[26] Chin CH, Chen SH, Wu HH, Ho CW, Ko MT, Lin CY. cytoHubba: identifying hub objects and sub-networks from complex interactome. BMC Systems Biology. 2014, 8(S4).
https://doi.org/10.1186/1752-0509-8-s4-s11

[27] Shannon P, Markiel A, Ozier O, et al. Cytoscape: A Software Environment for Integrated Models of Biomolecular Interaction Networks. Genome Research. 2003, 13(11): 2498-2504.
https://doi.org/10.1101/gr.1239303

[28] Bader GD, Hogue CW. BMC Bioinformatics. 2003, 4(1): 2.
https://doi.org/10.1186/1471-2105-4-2

[29] Huang DW, Sherman BT, Tan Q, et al. DAVID Bioinformatics Resources: expanded annotation database and novel algorithms to better extract biology from large gene lists. Nucleic Acids Research. 2007, 35(S2): W169-W175.
https://doi.org/10.1093/nar/gkm415

[30] Pawar SS, Rohane SH. Review on Discovery Studio: An important Tool for Molecular Docking. Asian Journal Of Research in Chemistry. 2021, 14(1): 1-3. https://doi.org/10.5958/0974-4150.2021.00014.6

[31] Jin X, Awale M, Zasso M, Kostro D, Patiny L, Reymond JL. PDB-Explorer: a web-based interactive map of the protein data bank in shape space. BMC Bioinformatics. 2015, 16(1). https://doi.org/10.1186/s12859-015-0776-9

[32] Gagnon JK, Law SM, Brooks CL. Flexible CDOCKER: Development and application of a pseudo-explicit structure-based docking method within CHARMM. Journal of Computational Chemistry. 2015, 37(8): 753-762. https://doi.org/10.1002/jcc.24259

[33] Zheng J, Yao L, Zhou Y, et al. A novel function of NLRP3 independent of inflammasome as a key transcription factor of IL-33 in epithelial cells of atopic dermatitis. Cell Death and Disease. 2021, 12(10). https://doi.org/10.1038/s41419-021-04159-9

[34] Dehne N, Brüne B. HIF-1 in the inflammatory microenvironment. Experimental Cell Research. 2009, 315(11): 1791-1797. https://doi.org/10.1016/j.yexcr.2009.03.019

[35] Wu L, Zhang Q, Liang W, Ma Y, Niu L, Zhang L. Phytochemical Analysis Using UPLC-MSn Combined with Network Pharmacology Approaches to Explore the Biomarkers for the Quality Control of the Anticancer Tannin Fraction of Phyllanthus emblica L. Habitat in Nepal. Hu W, ed. Evidence-Based Complementary and Alternative Medicine. 2021, 2021: 1-19. https://doi.org/10.1155/2021/6623791

[36] Yang B, Kortesniemi M, Liu P, Karonen M, Salminen JP. Analysis of Hydrolyzable Tannins and Other Phenolic Compounds in Emblic Leafflower (Phyllanthus emblica L.) Fruits by High Performance Liquid Chromatography–Electrospray Ionization Mass Spectrometry. Journal of Agricultural and Food Chemistry. 2012, 60(35): 8672-8683. https://doi.org/10.1021/jf302925v

[37] Jafarinia M, Sadat Hosseini M, kasiri N, et al. Quercetin with the potential effect on allergic diseases. Allergy, Asthma and Clinical Immunology. 2020, 16(1). https://doi.org/10.1186/s13223-020-00434-0

[38] Lee HN, Shin SA, Choo GS, et al. Anti-inflammatory effect of quercetin and galangin in LPS-stimulated RAW264.7 macrophages and DNCB-induced atopic dermatitis animal models. International Journal of Molecular Medicine. Published online November 29, 2017. https://doi.org/10.3892/ijmm.2017.3296

[39] Mehrbani M, Choopani R, Fekri A, Mehrabani M, Mosaddegh M, Mehrabani M. The efficacy of whey associated with dodder seed extract on moderate-to-severe atopic dermatitis in adults: A randomized, double-blind, placebo-controlled clinical trial. Journal of Ethnopharmacology. 2015, 172: 325-332. https://doi.org/10.1016/j.jep.2015.07.003

[40] Gendrisch F, Esser PR, Schempp CM, Wölfle U. Luteolin as a modulator of skin aging and inflammation. BioFactors. 2020, 47(2): 170-180. https://doi.org/10.1002/biof.1699

[41] Kempuraj D, Thangavel R, Kempuraj DD, et al. Neuroprotective effects of flavone luteolin in neuroinflammation and neurotrauma. BioFactors. 2020, 47(2): 190-197. https://doi.org/10.1002/biof.1687

[42] Bai J, Zhang Y, Tang C, et al. Gallic acid: Pharmacological activities and molecular mechanisms involved in inflammation-related diseases. Biomedicine and Pharmacotherapy. 2021, 133: 110985. https://doi.org/10.1016/j.biopha.2020.110985

[43] Chan HHL, Ng T. Traditional Chinese Medicine (TCM) and Allergic Diseases. Current Allergy and Asthma Reports. 2020, 20(11). https://doi.org/10.1007/s11882-020-00959-9

[44] Diao Q, Liu Y. Diagnosis and Treatment of Hang Eczema: a Chinese Expert Consensus Statement. Chinese Journal of Dermatovenereology of Integrated Traditional and Western Medicine, 2021, 20(5): 517-521.

[45] Shi DH, Dai YP, Su BZ, et al. Study on internal and external quality control methods of Platycladi Cacumen Carbonisata based on QAMS and color recognition. Zhongguo Zhong yao za zhi = Zhongguo zhongyao zazhi = China journal of Chinese materia medica, 2020, 45(24): 5996-6002.

[46] Darby IA, Hewitson TD. Hypoxia in tissue repair and fibrosis. Cell and Tissue Research. 2016, 365(3): 553-562. https://doi.org/10.1007/s00441-016-2461-3

[47] Manresa MC, Smith L, Casals-Diaz L, et al. Pharmacologic inhibition of hypoxia-inducible factor (HIF)-hydroxylases ameliorates allergic contact dermatitis. Allergy. 2018, 74(4): 753-766. https://doi.org/10.1111/all.13655

[48] Sun L, Liu W, Zhang L juan. The Role of Toll-Like Receptors in Skin Host Defense, Psoriasis, and Atopic Dermatitis. Journal of Immunology Research. 2019, 2019: 1-13. https://doi.org/10.1155/2019/1824624